PHYSICAL REVIEW B VOLUME 61, NUMBER 4 15 JANUARY 2000-II

Enhanced phonon-assisted photoluminescence in InAs/GaAs parallelepiped quantum dots

V. M. Fomin,* V. N. Gladilin,† S. N. Klimin,† and J. T. Devreese‡
Theoretische Fysica van de Vaste Stof, Departement Natuurkunde, Universiteit Antwerpen (U.I.A.), Universiteitsplein 1, B-2610 Antwerpen-Wilrijk, Belgium

P. M. Koenraad and J. H. Wolter
COBRA Inter-University Research Institute, Eindhoven University of Technology, NL-5600 MB Eindhoven, The Netherlands

(Received 16 September 1999)

We analyze the phonon-assisted photoluminescence due to the intraband transitions of an electron between the size-quantized states in rectangular parallelepiped InAs quantum dots (''quantum bricks'') embedded into GaAs. The phonon-assisted photoluminescence is strongly enhanced by two processes. First, the efficiency of the electron-phonon interaction in an individual quantum dot is enhanced in small dots. Second, we find that the ratio between intensities of the zero-phonon line and one-phonon line in the photoluminescence spectrum is efficiently controlled both by the shape and the size distribution of those quantum dots.

Advances in the synthesis of semiconductor nanocrystals have stimulated interest in novel fabrication methods which can provide quantum dots of different geometry, like E-beam lithography which allows the production of optically active nanostructures down to 100 nm.[1] Recently, a new technology has been developed: the atomic force microscope (AFM) mediated direct oxidation of semiconductor surfaces.[2] By this method, the surface of shallow Ga[Al]As heterostructures has been patterned; in particular, antidot lattices have been produced with periods down to 250 nm. Direct local anodic oxidation of high-mobility transistors has been shown to provide an effective *in situ* control of patterning semiconductor nanostructures. By optimization of the writing speed, the tip voltage and the control of the humidity, this method is expected to enable a reduction of the oxide line width below 20 nm. In our opinion, the AFM-based method seems promising for fabrication of smaller optically active nanostructures.

Optical characterization has been successfully applied to semiconductor nanostructures, see, e.g., reports on multiphonon photoluminescence[3,4] and Raman scattering[5,6] of nanosize quantum dots. A considerable enhancement of the phonon-assisted interband transition probabilities in the optical spectra of spherical quantum dots, even with relatively weak electron-phonon coupling strength, has been explained to be due to nonadiabaticity of the exciton-phonon systems.[7,8] Recently, the observed photoluminescence spectra in InAs/GaAs self-assembled quantum dots were attributed to a giant efficiency of the Fröhlich interaction between a strain-induced polarized exciton and the longitudinal optical (LO) phonons.[9] In nanostructures where the motion of charge carriers is confined to a small volume, the efficiency of the phonon-assisted interband transition processes greatly increases in the regime of strong size quantization, $\ell \leqslant R_B$, where ℓ is a characteristic size of a nanostructure and R_B is the exciton Bohr radius. In bulk InAs, the electron-phonon interaction is very weak: the Fröhlich coupling constant is $\alpha_{\mathrm{InAs}} \approx 0.052$.[10] Since the exciton Bohr radius in InAs is ≈ 35 nm, the strong size quantization regime occurs even in relatively large InAs quantum dots with characteristic sizes of the order of 10 nm, hopefully attainable by AFM structuring.

For optical examination in the far-infrared region, high-power tunable free-electron lasers are now available. These free-electron lasers are tunable over a wide spectral region. As an example, the FELIX (Free-Electron Laser for Infrared eXperiments) facility provides an extended wavelength range from 4.5 to 200 μm.[11] We propose to use this type of facility to study the intraband transitions in quantum dots. For optical intraband transitions in quantum dots, the condition of strong size quantization is $\ell \leqslant R_p$, where $R_p \equiv (\hbar/m_b\omega_{\mathrm{LO}})^{1/2}$ is a polaron radius, m_b is the band electron mass, ω_{LO} is the bulk LO-phonon frequency. In InAs quantum dots, the strong size quantization regime for intraband transitions is determined by the value $R_p \approx 10.6$ nm. This is again in the aforementioned size range of the quantum dots.

We analyze here the phonon-assisted photoluminescence in rectangular parallelepiped InAs quantum dots embedded into GaAs (''quantum bricks'' with sizes ℓ_x, ℓ_y, ℓ_z) due to the intraband transitions of an electron between the size-quantized states:

$$|kmn\rangle = \sqrt{\frac{8}{\ell_x \ell_y \ell_z}} \sin\left(\frac{\pi k}{\ell_x} x\right) \sin\left(\frac{\pi m}{\ell_y} y\right) \sin\left(\frac{\pi n}{\ell_z} z\right), \tag{1}$$

where k, m, n are positive integers.

Optical-phonon eigenmodes and the Hamiltonian of the electron-phonon interaction are obtained within the multimode dielectric model,[12] which takes into account both electrostatic and mechanical boundary conditions for the ionic displacement vector (see Ref. 13), as well as the phonon spatial dispersion in the bulk. This model has been recently used for the interpretation of optical spectra of spherical quantum dots.[7,8] Here, we briefly recall only the main ingredients of this model. When the phonon dispersion is relatively weak, vibrational eigenmodes in quantum dots are subdivided into the bulklike and interface ones. Within the multimode dielectric model,[12] at the boundaries, the components of the basis vectors normal to the boundary have nodes while the tangential components have extrema. Another distinctive feature of the multimode dielectric model[12] is that it

explicitly takes into account the finite number of vibrational modes in a quantum dot. The results of the multimode dielectric model have been shown to be in qualitative accordance with those obtained in microscopic models.[14,15] In the case of dispersive phonons, the vibrational modes in a quantum dot cannot be classified into bulklike or interface modes, but are their *hybrids*. The mixing between bulklike and interface vibrations is enhanced when decreasing the size of a quantum dot.

We calculate the photoluminescence spectra of quantum dots within the approach of Ref. 7 extended to the case of dispersive phonons, and consider optical transitions between two lowest size quantization states.[16] In this approximation, the probabilities of the optical transitions accompanied by emission of K phonons (both in the light absorption and in the photoluminescence) are

$$W_K(\Omega)=\frac{4\pi^2e^2\Omega}{n^2(\Omega)\hbar}e^{-S}\sum_f|\langle f|(\mathbf{n}\cdot\mathbf{r})|i\rangle|^2 \times\sum_{\{K_\nu\}:\Sigma_\nu K_\nu=K}\left(\prod_\nu\frac{S_\nu^{K_\nu}}{K_\nu!}\right) \times\delta_\gamma\left(\mp\tilde{\omega}_{fi}+\sum_\nu K_\nu\omega_\nu\pm\Omega\right), \tag{2}$$

where the sum is over all sets of integers K_ν which satisfy the condition $\Sigma_\nu K_\nu=K$; $n(\Omega)$ is the refractive index of the host medium, e is the electron charge. The upper (lower) sign corresponds to the emission (absorption) of a photon with frequency Ω. $\langle f|(\mathbf{n}\cdot\mathbf{r})|i\rangle$ is the matrix element of the transition between the initial ($|i\rangle$) and final ($|f\rangle$) states, $\mathbf{n}$ is the light polarization unit vector, and $\tilde{\omega}_{fi}$ is the Franck-Condon transition frequency. The excited electron state $|f\rangle$ is assumed to be homogeneously broadened with the linewidth γ:

$$\delta_\gamma(\Omega)\equiv\frac{\gamma}{\pi(\Omega^2+\gamma^2)}. \tag{3}$$

The partial Huang-Rhys parameter, related to the νth phonon mode with frequency ω_ν, is

$$S_\nu=\frac{|\langle i|\gamma_\nu|i\rangle-\langle f|\gamma_\nu|f\rangle|^2}{\hbar^2\omega_\nu^2}, \tag{4}$$

where γ_ν is the amplitude of the electron-phonon interaction, and the total Huang-Rhys parameter is $S=\Sigma_\nu S_\nu$.

In this paper, we consider photoluminescence spectra of the Gaussian ensemble of quantum dots

$$\mathcal{N}(l_x,l_y,l_z)=\frac{1}{(2\pi)^{3/2}V\sigma^3}\exp\left\{-\sum_{p=x,y,z}\frac{(l_p-\langle l_p\rangle)^2}{2\sigma^2\langle l_p\rangle^2}\right\}, \tag{5}$$

where σ is the half-width of the distribution over sizes, so that the relative size dispersion $\Delta=2\sigma$. For the monochromatic excitation radiation with the frequency Ω_{exc}, the absorption occurs only when the equation

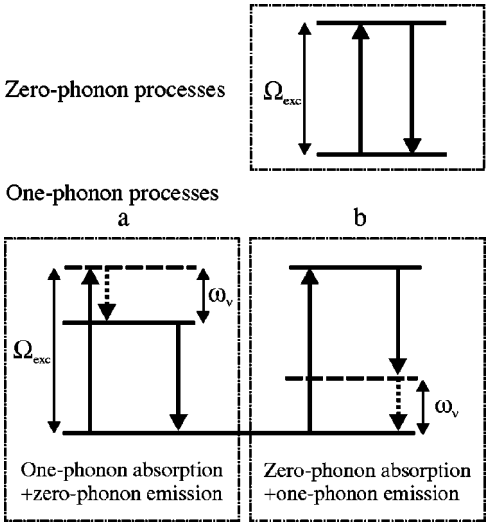

FIG. 1. Transition scheme for the light absorption under the excitation by the radiation of frequency Ω_{exc} (arrows up) and for the subsequent luminescence (arrows down) in quantum dots. One-phonon-assisted photoluminescence processes, accompanied by the emission of a phonon with a frequency ω_ν (dotted arrows down) are shown for the quantum dots of two different sizes: (a) larger dots, where the absorption of a photon is accompanied by the emission of a phonon, and (b) smaller dots, where the emission of a photon is accompanied by the emission of a phonon. The dashed lines denote the excited states of the electron-phonon system with one phonon of frequency ω_ν.

$$\tilde{\omega}_{fi}(\ell_x,\ell_y,\ell_z)+\sum_\nu K_\nu\omega_\nu-\Omega_{exc}=0 \tag{6}$$

is satisfied. Equation (6) can be solved for different numbers $K_\nu=0,1,2\ldots$ of emitted phonons of different frequency. It follows, therefore, that quantum dots of different sizes can be excited by the radiation of one and the same frequency Ω_{exc}. As a result, the K-phonon band of the photoluminescence spectra contains peaks provided by various combinations of transitions with the light absorption accompanied by $N\leqslant K$ phonons, followed by the light emission with participation of $(K-N)$ phonons. In particular (see Fig. 1), the one-phonon photoluminescence peak occurs when a phonon is emitted during light absorption with the subsequent zero-phonon light emission (a), and a phonon is emitted during light emission after the zero-phonon absorption (b). Since the Franck-Condon transition frequency $\tilde{\omega}_{fi}$ is a decreasing function of sizes of a quantum dot, the former process involves quantum dots with larger sizes than the latter one does. This effect gives rise to the possibility of controlling the ratio between intensities of the one-phonon and zero-phonon photoluminescence by varying the excitation frequency.

Assuming that $\ell_x>\ell_y,\ell_z$, the two lowest size quantization states are $|111\rangle$ and $|211\rangle$. In this case, $\tilde{\omega}_{fi}$ is a function of ℓ_x only. The set of equations (6) transforms into two equations for the sizes $l_0(\Omega_{exc})$, corresponding to the zero-phonon excitation; and $l_{1,\nu}(\Omega_{exc})$, corresponding to the one-phonon excitation:

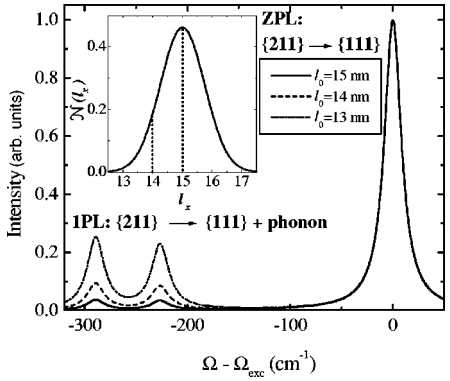

FIG. 2. Photoluminescence spectra of an ensemble of InAs/GaAs parallelepiped quantum dots with parameters $\langle \ell_x \rangle = 15$ nm, $\langle \ell_y \rangle = 10$ nm, $\langle \ell_z \rangle = 2$ nm, $\Delta \ell_p \langle \ell_p \rangle = 0.1$ $(p = x,y,z)$ for $\Omega_{exc} = 1756$ cm^{-1} ($l_0 = 15.0$ nm); $\Omega_{exc} = 2016$ cm^{-1} ($l_0 = 14.0$ nm); $\Omega_{exc} = 2338$ cm^{-1}($l_0 = 13.0$ nm). Distribution of quantum dots over ℓ_x is shown in the inset. The dotted lines denote the sizes of dots l_0 active in the zero-phonon light absorption at different excitation frequencies $\Omega_{\rm exc}$. In this and subsequent figures, the maximum intensity for the zero-phonon line is chosen as unit intensity.

$$\tilde{\omega}_{fi}(l_0) - \Omega_{exc} = 0,$$

$$\tilde{\omega}_{fi}(l_{1,\nu}) + \omega_\nu - \Omega_{exc} = 0. \tag{7}$$

It follows from the above-mentioned behavior of $\tilde{\omega}_{fi}$ as a function of sizes of a quantum dot, that $l_{1,\nu}(\Omega_{exc}) > l_0(\Omega_{exc})$. The zero-phonon and one-phonon photoluminescence spectra are given by the expression [which results from Eq. (34) of Ref. 7]

$$I(\Omega) = \mathcal{N}(l_0(\Omega_{exc}))\delta_\gamma(\Omega - \Omega_{exc}) + \sum_\nu [\mathcal{N}(l_0(\Omega_{exc}))S_\nu(l_0(\Omega_{exc})) + \mathcal{N}(l_{1,\nu}(\Omega_{exc}))S_\nu(l_{1,\nu}(\Omega_{exc}))]\delta_\gamma(\Omega - \Omega_{exc} + \omega_\nu). \tag{8}$$

The results of the calculation of the photoluminescence spectra in Gaussian ensembles of InAs/GaAs quantum dots are presented in Figs. 2 to 4. The homogeneous linewidth γ is taken to be 10 cm^{-1}.

Comparing curves shown in Fig. 2, one can see that for an increasing frequency Ω_{exc} the excitation is shifted to smaller quantum dots, i.e., $l_0(\Omega_{exc})$ becomes smaller. By shifting the excitation to these smaller quantum dots, the intensity of the zero-phonon peak I_0 decreases more quickly than the intensity of the one-phonon peak I_1, so that the ratio I_1/I_0 rises. This fact can be explained by the structure of Eq. (8): for $l_0 < \langle \ell_x \rangle$, the ratio of the terms in between the square brackets to the quantity which determines the intensity of the zero-phonon peak, $\mathcal{N}(l_0(\Omega_{exc}))$, rises when increasing the excitation frequency Ω_{exc}, i.e., when excitation is shifted to smaller quantum dots. Under the condition $\mathcal{N}(l_{1,\nu}(\Omega_{exc})) > \mathcal{N}(l_0(\Omega_{exc}))$, the dominant contribution to the one-phonon peak intensity is due to the processes shown in Fig. 1(a) that occur in the quantum dots of size $l_{1,\nu}(\Omega_{exc})$.

Figures 2 and 3 allow one to compare photoluminescence spectra for two Gaussian ensembles of quantum dots with the

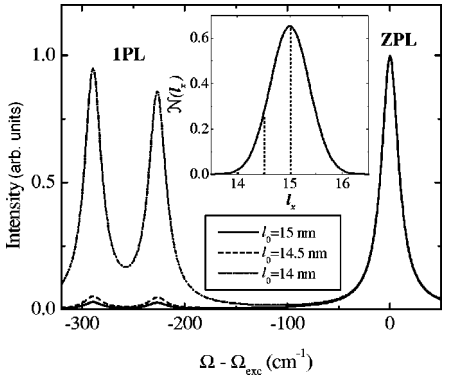

FIG. 3. Photoluminescence spectra of an ensemble of InAs/GaAs parallelepiped quantum dots with $\langle \ell_x \rangle = 15$ nm, $\langle \ell_y \rangle = 10$ nm, $\langle \ell_z \rangle = 2$ nm, $\Delta \ell_p \langle \ell_p \rangle = 0.05$ $(p = x,y,z)$ for $\Omega_{exc} = 1756$ cm^{-1} ($l_0 = 15.0$ nm); $\Omega_{exc} = 1880$ cm^{-1} ($l_0 = 14.5$ nm); $\Omega_{exc} = 2016$ cm^{-1} ($l_0 = 14.0$ nm). Distribution of quantum dots over ℓ_x is shown in the inset. The dotted lines have the same meaning as those in Fig. 2.

relative size dispersion $\Delta = 0.1$ (10%) and $\Delta = 0.05$ (5%), respectively. The aforementioned effect of the enhancement of the factor I_1/I_0, when increasing the excitation frequency, is more pronounced for a narrow size distribution than for a wide one. For the plots shown in Fig. 3, I_1/I_0 occurs to be close to 1. This means a substantial *enhancement* of the efficiency of the electron-phonon interaction in the quantum dots [compared to the bulk InAs or GaAs (Ref. 17)] in conjunction with statistical effects in the ensemble of quantum dots.

In all figures, the one-phonon photoluminescence band consists of two peaks which correspond to hybrid InAs-like phonon modes (at ≈ 230 cm^{-1}) and to hybrid GaAs-like phonon modes (at ≈ 285 cm^{-1}). The ratio between the intensities of these two peaks depends on the shape of a quantum dot. When comparing photoluminescence spectra for ensembles of quantum dots with $\langle \ell_y \rangle = 10$ nm (Fig. 3) and $\langle \ell_y \rangle = 3$ nm (Fig. 4) (where the other two sizes $\langle \ell_x \rangle = 15$ nm and $\langle \ell_z \rangle = 2$ nm have been fixed for both cases) we can

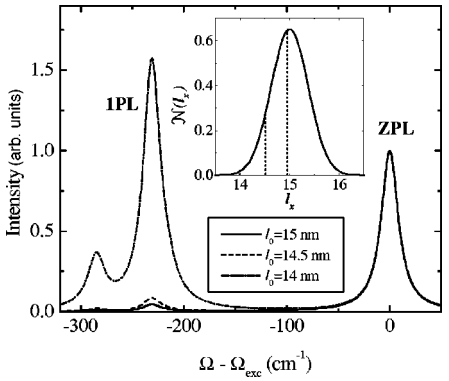

FIG. 4. Photoluminescence spectra of an ensemble of InAs/GaAs parallelepiped quantum dots with $\langle \ell_x \rangle = 15$ nm, $\langle \ell_y \rangle = 3$ nm, $\langle \ell_z \rangle = 2$ nm, $\Delta \ell_p \langle \ell_p \rangle = 0.05$ $(p = x,y,z)$ for $\Omega_{exc} = 1756$ mcm^{-1} ($\ell_0 = 15.0$ nm); $\Omega_{exc} = 1880$ cm^{-1} ($l_0 = 14.5$ nm); $\Omega_{exc} = 2016$ cm^{-1} ($l_0 = 14.0$ nm). Distribution of quantum dots over ℓ_x is shown in the inset. The dotted lines have the same meaning as those in Fig. 2.

observe that the peaks due to GaAs-like phonons are relatively more pronounced for flatter dots than for more elongated dots.

In conclusion, we have shown that the ratio between intensities of the one-phonon line and the zero-phonon line in a photoluminescence spectrum largely depends on the size of the individual quantum dots and on the size distribution in the ensemble of quantum dots. The relative enhancement of phonon-assisted photoluminescence for narrow size distributions provides an effective method to characterize vibrational states in single InAs/GaAs quantum dots. If the optical transitions between the confined electron states in quantum dots can be seen, then there is good reason to expect phonon-assisted transitions due to hybrid phonons to be equally observed.

The authors thank E. P. Pokatilov for fruitful discussions. This work has been supported by the BOF NOI (UA-UIA), IUAP, FWO-V., Projects Nos. G.0287.95, G.0193.97 and the W.O.G. WO.025.99N (Belgium), and the PHANTOMS research network.

*Also at Technische Universiteit Eindhoven, P.O. Box 513, 5600 MB Eindhoven, The Netherlands. Permanent address: Department of Theoretical Physics, State University of Moldova, Strada A. Mateevici 60, MD-2009 Kishinev, Republic of Moldova.

†Permanent address: Department of Theoretical Physics, State University of Moldova, Strada A. Mateevici 60, MD-2009 Kishinev, Republic of Moldova.

‡Also at Universiteit Antwerpen (RUCA), Groenenborgerlaan 171, B-2020 Antwerpen, Belgium and Technische Universiteit Eindhoven, P.O. Box 513, 5600 MB Eindhoven, The Netherlands.

[1] B. Hübner, B. Jacobs, Ch, Gréus, R. Zengerle, and A. Forchel, J. Vac. Sci. Technol. B **12**, 3658 (1994); P. J. Klar, D. Wolverson, J. J. Davies, W. Heimbrodt, M. Happ, and T. Henning, Phys. Rev. B **57**, 7114 (1998).

[2] R. Held, T. Vancura, T. Heinzel, K. Ensslin, M. Holland, and W. Wegscheider, Appl. Phys. Lett. **73**, 262 (1998); in *Proceedings of the 24th International Conference on the Physics of Semiconductors*, edited by D. Gershoni (World Scientific, Singapore, 1999), (Tul-D4).

[3] V. Jungnickel and F. Henneberger, J. Lumin. **70**, 238 (1996).

[4] D. J. Norris, Al. L. Efros, M. Rosen, and M. G. Bawendi, Phys. Rev. B **53**, 16 347 (1996).

[5] G. Scamarcio, V. Spagnolo, G. Ventruti, M. Lugará, and G. C. Righini, Phys. Rev. B **53**, R10 489 (1996).

[6] T. D. Krauss and F. W. Wise, Phys. Rev. B **55**, 9860 (1997).

[7] V. M. Fomin, V. N. Gladilin, J. T. Devreese, E. P. Pokatilov, S. N. Balaban, and S. N. Klimin, Phys. Rev. B **57**, 2415 (1998).

[8] V. M. Fomin, E. P. Pokatilov, J. T. Devreese, S. N. Klimin, V. N. Gladilin, and S. N. Balaban, Solid-State Electron. **42**, 1309 (1998).

[9] A. W. E. Minnaert, A. Yu. Silov, W. van der Vleuten, J. E. M. Haverkort, J. H. Wolter, A. García-Cristóbal, V. N. Gladilin, V. M. Fomin, and J. T. Devreese, in: *Proceedings of the 24th International Conference on the Physics of the Semiconductors*, (Ref. 2), (Mo-P139).

[10] E. Kartheuser, in *Polarons in Ionic Crystals and Polar Semiconductors*, edited by J. T. Devreese (North-Holland, Amsterdam, 1972), p. 726.

[11] D. A. Jaroszynski, R. Prazeres, F. Glotin, J. M. Ortega, D. Oepts, A. F. G. van der Meer, G. M. H. Knippels, and P. W. van Amersfoort, Phys. Rev. Lett. **74**, 2224 (1995).

[12] S. N. Klimin, E. P. Pokatilov, and V. M. Fomin, Phys. Status Solidi B **190**, 441 (1995).

[13] V. M. Fomin and E. P. Pokatilov, in *Proceedings of the Fourth International Conference on the Formation of Semiconductor Interfaces* (World Scientific, Singapore, 1994), p. 704.

[14] K. Huang and B. Zhu, Phys. Rev. B **38**, 13 377 (1988).

[15] E. Molinari, S. Baroni, P. Giannozzi, and S. de Gironcoli, Phys. Rev. B **45**, 4280 (1992).

[16] Taking into account that, generally speaking, the parallelepiped quantum dots do not provide degenerate electron states, nonadiabatic effects are not analyzed here. A possible role of nonadiabatic optical transitions in the parallelepiped quantum dots will be discussed elsewhere.

[17] P. A. Wolff, Phys. Rev. **171**, 436 (1968).